Proc. Natl. Acad. Sci. USA
Vol. 79, pp. 2564–2568, April 1982
Biophysics

Preparation of a spectral probe derivative of the hemocyanin biopolymer: Effects of allosteric interactions on the coupled binuclear copper active site

(cooperativity in oxygen binding/mixed valence copper electron paramagnetic resonance/calcium binding)

YEONG TSYR HWANG AND EDWARD I. SOLOMON*

Department of Chemistry, Massachusetts Institute of Technology, Cambridge, Massachusetts 02139

Communicated by John I. Brauman, January 25, 1982

ABSTRACT **A series of derivatives for both the arthropod and mollusc hemocyanin biopolymers has been prepared; the derivatives contain a small fraction of electron paramagnetic resonance-detectable half-met [Cu(II) Cu(I)] sites dispersed among the non-detectable oxy binuclear copper active sites. Upon deoxygenation, large changes in the electron paramagnetic resonance signal of these half-met spectral probe derivatives are observed, which are further adjusted by the heterotropic effectors Ca^{2+} and H^+. The active site structural changes indicated by these spectral changes as the hemocyanins go from a relaxed to a tensed quaternary structure are then discussed.**

Hemocyanins, the oxygen transport proteins in the hemolymph of molluscs and arthropods, reversibly bind dioxygen with a stoichiometry of one dioxygen per two copper ions. Under physiological conditions, the hemocyanins are present as highly aggregated biopolymers with a molecular architecture that differs dramatically between the two phyla. For the arthropods, a single subunit has a molecular weight of ≈70,000 and contains one binuclear copper active site. At pH values below 8 and in the presence of Ca^{2+}, these subunits aggregate into one, two, four, and in the case of *Limulus polyphemus*, up to eight hexamers. Alternatively, the smallest subunit in the molluscs contains about eight binuclear copper active sites (domains) covalently linked in a single polypeptide chain of ≈400,000 daltons. In the mollusc *Busycon canaliculatum*, at pH less than 8, twenty chains aggregate to form a whole molecule that contains ≈160 active sites and appears as a cylindrical barrel under the electron microscope. When aggregated, the hemocyanins are highly cooperative in their oxygen binding, with Hill coefficients dependent on species, pH, and the presence of divalent cations (1, 2).

In general, current thermodynamic and kinetic theories of oxygen binding to the hemocyanins parallel [with small modifications (3, 4)] the allosteric model of hemoglobin. Deoxyhemocyanin has a "tensed" quaternary structure with a low oxygen affinity. Initial binding of oxygen to a limited number of active sites alters the successive oxygen affinities of the remaining sites by a ligand-induced conformational change of the protein (5) (i.e., oxygen is a homotropic effector); this results in the oxyhemocyanin having a "relaxed" quaternary structure with a high oxygen affinity. Protons and divalent cations act as heterotropic effectors, which, depending upon the species, stabilize either the tensed or relaxed quaternary structure.

For hemoglobin, through both protein crystallography (6) and the detailed study of iron prophyrin model complexes (7), significant advances have been made in the development of a structural model that accounts for the active site changes related to these changes in oxygen affinity. Two basic spectroscopic approaches have been taken to relate this mechanical model to the hemoglobin tetramer. One approach involves the preparation of valence hybrids in which either the α or the β chains contain iron(III) sites (met sites) and the other sites can be deoxygenated (8, 9); the second involves the study of spectral effects on oxy-, deoxy-, and methemoglobin active sites induced by heterotropic effectors (inositol hexaphosphate or low pH) (10) that shift the equilibrium from the relaxed to the tensed quaternary structure. No analogous attempts have been made to correlate changes in the hemocyanin active site with change in protein quaternary structure.

Our development of a spectroscopically effective structural model for the oxyhemocyanin active site involved the preparation of a series of protein derivatives (Fig. 1) that enable the active site to be systematically varied. Spectral study of these derivatives resulted in the structural model shown at the bottom of Fig. 1 (11, 12). Binding oxygen to deoxyhemocyanin [which is structurally the least well characterized of all derivatives (see discussion in *Preliminary Structural Implications*) but contains a binuclear cuprous site] is generally believed to result in a μ-dioxoperoxide bound to two tetragonal copper(II)s that are antiferromagnetically coupled through the endogenous bridge (RO^-). Thus, both deoxy and oxy forms are not EPR detectable. If a small amount (≈10%) of one of the EPR-detectable derivatives in Fig. 1 could be dispersed within the oxyhemocyanin biopolymer, then the effects on the active site of changes in quaternary structure induced by deoxygenation could be probed through changes in the EPR spectrum. The stability, rich chemistry, and spectroscopy of the half-met derivatives (13) makes this derivative the ideal probe. We report here the preparation of this spectral probe (SP) derivative for both the arthropod and mollusc hemocyanin biopolymers; further, we demonstrate that deoxygenation of dominant oxy sites induces large changes in the half-met spectral probe (which are adjusted by the heterotropic effectors Ca^{2+} and H^+) and discuss at a preliminary level the structural changes indicated by these spectral changes.

MATERIALS AND METHODS

Hemolymph, obtained from *Busycon canaliculatum* by foot puncture, was centrifuged at 27,000 × *g* for 20 min to remove insoluble materials. The clear supernatant fluid was then centrifuged at 48,000 × *g* for 4 or 9 hr. The hemocyanin of *Limulus polyphemus* was collected by heart puncture, then centrifuged

The publication costs of this article were defrayed in part by page charge payment. This article must therefore be hereby marked "*advertisement*" in accordance with 18 U. S. C. §1734 solely to indicate this fact.

Abbreviation: SP, spectral probe.

* To whom reprint requests should be addressed at the present address: Dept. of Chemistry, Stanford University, Stanford, CA 94305.

immediately at 27,000 × g for 20 min to remove the coagulated cells and large particles. The clear supernatant fluid was centrifuged at 120,000 × g for 4 hr with a Beckman model L ultracentrifuge. Both dark blue pellets were redissolved in 0.1 M potassium phosphate buffer, pH 6.3, to a protein concentration of 0.7–1.0 mM.

All EPR spectra were obtained with a Varian E-9 spectrometer (X-band) on solution samples frozen at liquid nitrogen temperature. Protein concentration was determined by absorbance at 278 nm and oxy content by absorbance at 345 nm with a Cary 14 spectrophotometer. Deoxy proteins were prepared by repeated evacuation and addition of purified nitrogen gas that had been bubbled through a chromous solution. Electron microscopy specimens were prepared by negative staining with phosphotungstic acid and viewed in a Jeol 100B electron microscope at an accelerating voltage of 80 kV with magnification of ×135,000.

RESULTS AND DISCUSSION

Preparative. The hemocyanin of *Limulus polyphemus* can be dissociated into subunits and separated into at least eight heterogeneous fractions. Because these fractions can be reassembled into a high molecular weight protein that is morphologically and functionally indistinguishable from the undissociated state (14), a straightforward pathway to the *Limulus* SP hemocyanin is provided. Initial attempts to prepare a *Limulus* half-met–N_3^- SP were performed by first deaggregating the oxyhemocyanin and half-met–N_3^- derivative into subunits, then mixing these two monomeric forms, and finally reassembling this mixture. When half-met–N_3^- is prepared (13) and dissociated into subunits by dialysis (at room temperature, pH 8.9, 0.052 M Tris/glycine buffer) in the presence of 0.01 M EDTA for 48 hr, the monomer is obtained but the N_3^- ligand is no longer bound to the active site. Because pH is known to have a profound effect on ligand binding to the half-met active site, it is likely that at high pH the N_3^- is displaced by OH^-. Fortunately, *Limulus* half-met–NO_2^- was found to be more stable, because the nitrite remains tightly bound to the active site over a large pH range. Therefore, both the half-met–NO_2^- and oxy hemocyanin were dissociated into subunits, as described above,

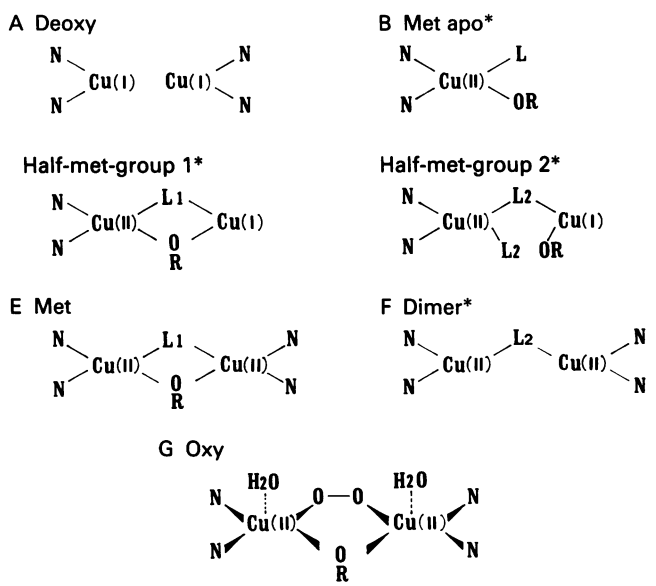

FIG. 1. Structural models of the active sites of hemocyanin derivatives. N, Protein ligand; OR, endogenous protein bridge; L, exogenous ligand; *, EPR-detectable.

and the monomeric units were mixed at 1:6 ratio (half-met–NO_2^-/oxy). The SP protein was reassembled in three steps according to Bijlholt *et al.* (14). During the reassembly procedure, a small amount of protein precipitates, but it is easily removed by centrifugation. The composition of the final SP derivative is defined by estimating its half-met–NO_2^- concentration by double integration of the EPR spectrum, and the content of oxy is calculated from the absorption peak at 345 nm in the optical spectrum. At this point, we had ≈7 ± 1% half-met–NO_2^- and about 93 ± 4% oxy active sites in this *Limulus* half-met–NO_2^- SP. The reassembled SP protein was dialyzed against pH 7.0, 0.1 M phosphate buffer and the aggregation state of the *Limulus* SP hemocyanin was confirmed by ultracentrifugation. *Limulus* hemocyanin in the oxy form is very stable to ligand displacement of peroxide by excess N_3^- (15), and, likewise, half-met excess-N_3^- SP can be made by dialysis of this reassembled SP protein against 1,000-fold excess N_3^- without perturbing the oxy sites.

As mentioned in the Introduction, the aggregation pattern in *Busycon* hemocyanin is very different from that of *Limulus* hemocyanin. Domains obtained after proteolytic digestion and column chromatography maintain their oxygen-binding characteristics but cannot be reassembled into the native high molecular weight form. Therefore, an alternative pathway was necessary for the preparation of the *Busycon* half-met spectral probe.

Deoxyhemocyanin can be oxidized by $NaNO_2$, at low pH and in the presence of ascorbic acid, to the half-met–NO_2^- form. This reaction proceeds through an EPR-nondetectable binuclear cupric (presumed to be met) intermediate (12), which further reduces to half-met–NO_2^- by NO in a kinetically slow step. Further, for *Busycon* hemocyanin, an EPR-nondetectable binuclear cupric met derivative can be prepared by ligand displacement of peroxide from oxy by either F^- or N_3^- (16). This met form is regenerable back to oxy by treatment with excess H_2O_2 (17). Our initial efforts to make the *Busycon* SP hemocyanin utilized these reactivity patterns. The *Busycon* hemocyanin was treated with excess $NaNO_2$ in the presence of ascorbic acid (pH 6.3, 0.1 M phosphate buffer) for 6 min. The reaction was stopped by titrating the solution with dilute KOH to pH 8.0. Fifteen percent half-met and 40% residual oxy sites were obtained in addition to the expected EPR-nondetectable intermediate. However, dialysis of this protein back into pH 6.3 phosphate and titration with H_2O_2 did not regenerate the remaining EPR-nondetectable intermediate to the oxy form. Deoxygenating the residual oxy sites of this protein does induce small changes in its half-met EPR signal. Thus, it appeared that the pH jump used to "turn off" the NO reaction damaged the protein. A Sephadex G-25 column, preequilibrated with pH 6.3, 0.1 M phosphate buffer, was alternatively used to remove the reagents and stop the $NaNO_2$ plus ascorbate reaction, but H_2O_2 titration of this solution still failed to regenerate the met sites to the oxy form. This suggests that the "met" intermediate produced in this $NaNO_2$ reaction is different from the "H_2O_2-regenerable" met form obtained by ligand displacement of oxyhemocyanin. Finally, a protocol was determined that enables us to prepare a well-defined *Busycon* SP that contains only half-met and oxy sites. Met was prepared in pH 5.0, 0.1 M sodium acetate buffer by incubation at 37°C for 48 hr with 100-fold excess NaF and then dialyzed into pH 6.3, 0.1 M phosphate buffer. This met derivative was then converted to partial half-met–NO_2^- by addition of excess $NaNO_2$ and ascorbate. After 6 min the reaction was stopped by passing the protein solution through a Sephadex G-25 column. In this case, 15 ± 2% half-met was obtained along with 85% met form. The protein solution then was allowed to react with 20-fold excess H_2O_2. This

yielded 85 ± 4% oxyhemocyanin with no change in the SP half-met–NO_2^- EPR signal. The amount of half-met–NO_2^- site in the biopolymer was varied by varying the $NaNO_2$ reaction time.

Finally, half-met–X derivatives of the *Busycon* SP were prepared directly by dialysis of half-met–NO_2^- SP against buffer solutions containing 100-fold excess ligand for 16 hr (excess form) at 4°C, followed by dialysis against pH 7.0, 0.1 M phosphate buffer for 20 hr (nonexcess form). All the *Busycon* SP derivatives under various conditions were compared to native hemocyanin by electron microscopy and the results showed no obvious change in their aggregation state.

Homotropic Effects. A series of half-met derivatives have been prepared that exhibit very interesting chemistry and spectroscopy and have provided a great deal of structural insight into the hemocyanin active site (13). Briefly, it was found that all exogenous ligands remain extremely tightly bound to the [Cu(II) Cu(I)] site due to their bridging of the two copper ions. These exogenous ligands, however, can be divided into two groups on the basis of the coordination chemistry observed in excess ligand concentrations. Group 1 ligands (NO_2^-, F^-, Cl^-, Br^-, I^-, $CH_3CO_2^-$) bridge (13) the two coppers with a <4-Å Cu–Cu distance and coordinate only one tightly bound ligand to the site (i.e., there is no EPR spectral change in excess ligand). Group 2 ligands (N_3^-, SCN^-, CN^-) are capable of bridging with a >5-Å Cu–Cu distance and are found to bind a second ligand to the Cu(II) when in excess. Here, the group 2 ligand breaks the endogenous protein bridge RO^- shown in Fig. 1 and opens a second coordination position on the Cu(II). The pure half-met ligand substitution reactions of *Limulus* and *Busycon* hemocyanins were repeated in pH 7.0, 0.1 M phosphate buffer, and the EPR spectra are presented in Fig. 2 for comparison to the SP results that follow.

Limulus half-met excess N_3^- SP in pH 7.0, 0.1 M phosphate buffer has the EPR spectrum shown in Fig. 3, curve A-1. Comparison of this EPR spectrum with that in Fig. 2 indicates the presence of a mixture of a large amount of half-met excess N_3^-

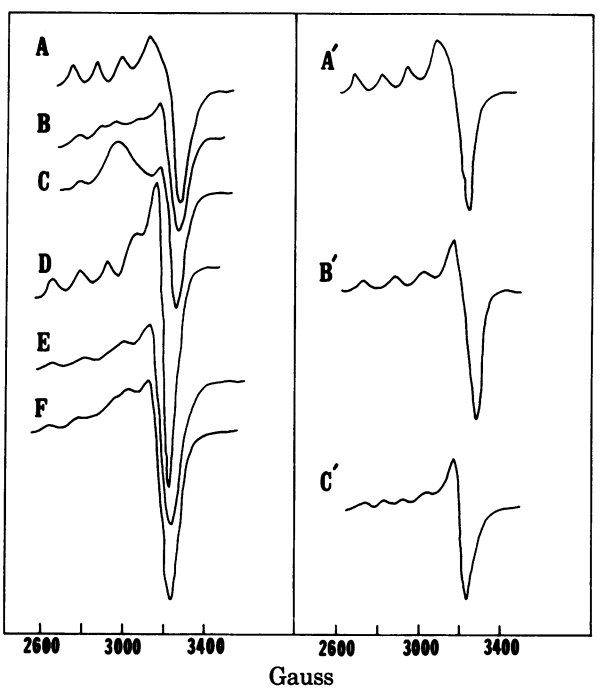

FIG. 2. EPR spectra of *Busycon* and *Limulus* half-met derivatives. *Busycon*: A, –NO_2^-; B, excess N_3^-; C, –N_3^-; D, –acetate; E, excess SCN^-; and F, –SCN^-. *Limulus*: A′, –NO_2^-; B′, excess N_3^-; and C′, –N_3^-.

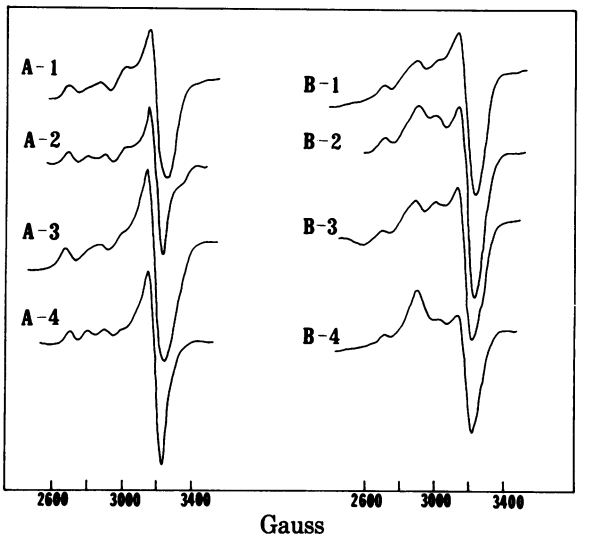

FIG. 3. EPR spectra. *Limulus* SP in 1000-fold excess N_3^-: A-1, oxy; A-2, deoxy; A-3, reoxy. A-4, *Limulus* half-met–N_3^- SP. *Busycon* SP in 100-fold excess N_3^-: B-1, oxy; B-2, deoxy; B-3, reoxy. B-4, *Busycon* half-met–N_3^- SP.

and a small amount of half-met–N_3^- (nonexcess) SP. Exhaustive dialysis of this half-met excess N_3^- SP against pH 7.0 phosphate buffer gives the half-met–N_3^- SP (Fig. 3, curve A-4), which looks quite similar to the pure half-met–N_3^- in Fig. 2. When the half-met excess N_3^- SP (Fig. 3, curve A-1) is deoxygenated, the EPR spectrum shows a striking change (Fig. 3, curve A-2), resulting in an EPR spectrum that is similar to the EPR signal of the half-met–N_3^- SP (Fig. 3, curve A-4). Upon reoxygenation of this deoxy SP, the blue color of the oxy sites appears immediately, whereas it takes several days to completely restore the original EPR spectrum of the half-met excess N_3^- SP (Fig. 3, curve A-3).

In the case of *Busycon* hemocyanin, the EPR spectrum of the half-met excess N_3^- SP is shown in Fig. 3, curve B-1, which indicates that a small amount of half-met–N_3^- form is also present by comparison to Fig. 2. Dialysis of this half-met excess N_3^- SP against pH 7.0, 0.1 M phosphate buffer gives the EPR spectrum in Fig. 3, curve B-4, analogous to the pure half-met–N_3^- shown in Fig. 2. When the half-met excess N_3^- SP protein is deoxygenated, the EPR spectrum changes dramatically (Fig. 3, curve B-2), indicating dominant conversion to the half-met nonexcess N_3^- SP form. Exposure of this deoxy SP to the air results in slow restoration of the oxy SP EPR signal (Fig. 3, curve B-3) and the immediate reappearance of the blue color of the oxy sites. The amount of half-met site present in the spectral probe was varied between 5% and 30%. All of these half-met excess N_3^- SPs show the same type of EPR spectral change upon deoxygenation; however, the degree of change decreases as the fraction of half-met sites is increased.

The behavior of the *Busycon* SP completely parallels that observed for the *Limulus* SP, both of which indicate that the second ligand at the half-met active site is eliminated upon deoxygenation of the dominant oxy sites. That is, the protein in the deoxy state has adapted a quaternary conformation that has a lower affinity for the excess ligand at the half-met probe sites.

For *Busycon* hemocyanin, these studies were extended to include a series of half-met–X SPs. The EPR spectra of oxy and deoxy *Busycon* half-met–N_3^- SP are shown in Fig. 4, curves A-1 and B-1. No obvious change is observed in this derivative (nor is a clear change observed in the EPR spectrum of the *Limulus*

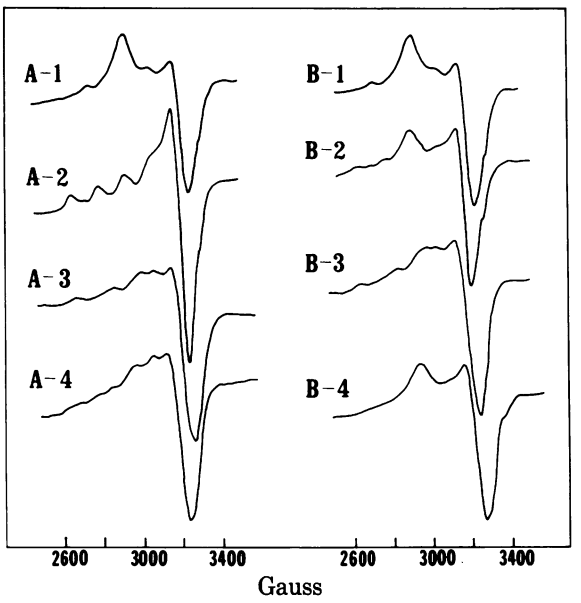

FIG. 4. EPR spectra of *Busycon* SP. Oxy SP: A-1, $-N_3^-$; A-2, -acetate; A-3, excess SCN^-; A-4, $-SCN^-$. Deoxy SP: B-1, $-N_3^-$; B-2, -acetate; B-3, excess SCN^-; B-4, $-SCN^-$.

half-met-N_3^- SP). *Busycon* half-met-acetate SP is made in pH 5.7, 0.1 M acetate buffer and then exhaustively dialyzed against pH 7.0 phosphate buffer. This SP shows the EPR signal given in Fig. 4, curve A-2. Upon deoxygenation, this half-met-acetate SP shows a pronounced change in its EPR spectrum (Fig. 4, curve B-2). Reoxygenation results in the rapid appearance of the blue color but fails to restore the EPR spectrum of the initial oxygenated SP. This apparent irreversibility in nonexcess ligand is not surprising in that the stability of the ligand binding to the oxy half-met-acetate SP form likely results from kinetic rather than thermodynamic factors. Dialysis of this reoxygenated half-met-acetate SP against pH 5.7, 0.1 M acetate followed by dialysis against pH 7.0 phosphate buffer results in the EPR spectrum of the original oxy half-met-acetate SP. Acetate was then replaced by SCN^- by using a 100-fold excess of SCN^-. The EPR spectrum of the resulting half-met excess SCN^- SP shows no obvious change between oxy and deoxy forms (Fig. 4, curves A-3 and B-3). The half-met-SCN^- SP, however, exhibits a pronounced change in its EPR spectrum (Fig. 4, curves A-4 and B-4) upon deoxygenation, providing a signal similar to that observed in the deoxy half-met-acetate SP. Also, analogous to half-met-acetate SP behavior, reoxygenation fails to restore the original oxy EPR signal. Dialysis of this reoxygenated half-met-SCN^- SP against a solution containing 100-fold excess SCN^- followed by dialysis against pH 7.0 phosphate buffer to remove excess SCN^- restores the original EPR spectrum of oxy half-met-SCN^- SP.

Thus the EPR signals of the half-met-acetate and half-met-SCN^- SP hemocyanins change upon deoxygenation to unique spectra (Fig. 4, curves B-2 and B-4) that are similar to the spectrum of half-met-N_3^-. This strongly suggests that there is a similar electronic structure for the active sites of the deoxy half-met-N_3^-, -acetate, and $-SCN^-$ SPs. For the case of half-met-N_3^-, this unique EPR signal is associated (13) with class 2 mixed valence behavior, in which the exogenous bridging ligand provides an effective pathway for delocalization of the extra electron from the Cu(I) to the Cu(II). Therefore, in addition to the elimination of the second ligand observed for the half-met excess N_3^- SP, the electronic and geometric structure of the binuclear copper site has been strongly affected upon going from the oxy to the deoxy conformation.

Heterotropic Effects. When purification of the *Busycon* hemocyanin has totalled more than 9 hr of centrifugation, the half-met excess N_3^- SP shows no obvious change in its EPR spectrum upon deoxygenation. However, when treated with 10 mM $CaCl_2$ (in the Tris/SO_4^{2-}, pH 7.0 buffer), the intersubunit interactions are restored and, in fact, enhanced (see oxy → deoxy, Fig. 5, curves A-1 and -2 → curves B-1 and -2). Reoxygenation of the Ca^{2+}-treated SP protein results in the reappearance of the blue color but fails to restore the oxy half-met excess N_3^- SP EPR signal. Further, a reduction in binding ability of the second ligand is observed [compare the EPR signal of the oxy SP form before (Fig. 5, curve A-1) and after (Fig. 5, curve A-2) the addition of Ca^{2+}] and all of the excess N_3^-, excess acetate, and excess SCN^- SP proteins produce half-met-aquo (13) instead of nonexcess forms by dialysis against buffer with 10 mM Ca^{2+}. Finally, in the presence of Ca^{2+}, the native oxy sites lose their oxygen upon sitting overnight at 4°C. All these observations suggest an allosteric effector role for Ca^{2+} that favors the low ligand affinity state of the protein. Alternatively, the addition of up to 0.4 M Na^+ does not restore the intersubunit interactions, because the EPR signal of half-met excess N_3^- SP does not change upon deoxygenation. Protons, however, do have a profound effect on the SP: the lower the pH value, the higher the excess ligand binding ability of the oxy half-met excess N_3^- site and the greater the change observed upon deoxygenation (Fig. 5, curves A-3, A-4, B-3, and B-4).

The addition of physiological levels of Ca^{2+} to *Busycon* hemocyanin has been shown to restore virtually all of the cooperativity in oxygen binding of the native blood, whereas Na^+ does not (18). From our studies of the SP hemocyanin, Ca^{2+} strongly enhances the sensitivity of the half-met SP to removal of O_2, whereas Na^+ has no effect. The pH effect on ligand binding in the half-met SP also parallels its effect on oxygen affinity: O_2 affinity decreases as pH increases. These results allow us to correlate the SP changes to the cooperativity in oxygen binding and may be interpreted in terms of a change in the equilibrium

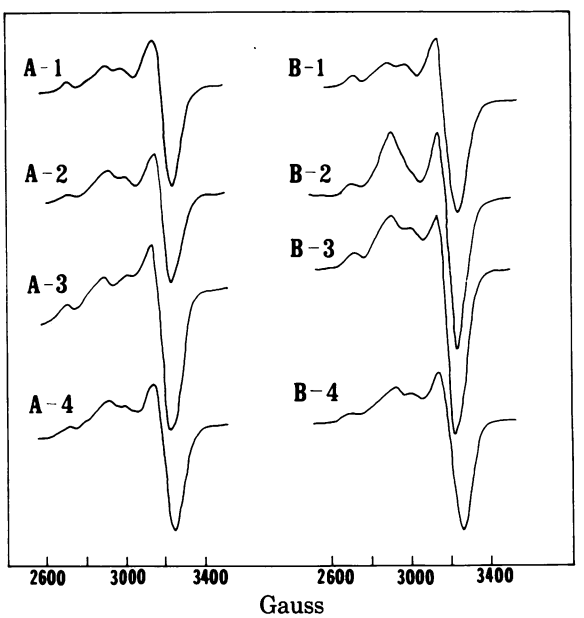

FIG. 5. EPR spectra of *Busycon* SP in 100-fold excess N_3^-. Nine hours of centrifugation without Ca^{2+}: A-1, oxy; B-1, deoxy. Nine hours of centrifugation with Ca^{2+}: A-2, oxy; B-2, deoxy. Four hours of centrifugation at pH 7.0: A-3, oxy; B-3, deoxy. Four hours of centrifugation at pH 8.0: A-4, oxy; B-4, deoxy.

between the tensed and relaxed conformations. Ca^{2+} lowers the oxygen affinity and, presumably, stabilizes the tensed conformation, whereas protons increase the oxygen affinity and stabilize the relaxed conformation below pH 8.0. This indicates that the active site environment not only changes upon binding of O_2 to other sites but also depends on the change in quaternary structure that is induced by other effectors.

Preliminary Structural Implications. The SP derivatives of both the mollusc and the arthropod hemocyanin biopolymers have clearly demonstrated that deoxygenation of adjacent sites (homotropic effect) and allosteric effectors (heterotropic effect) induce changes in the hemocyanin quaternary structure that result in significant spectral, and therefore structural, changes in the half-met probe site. The half-met changes upon going to this tensed quaternary structure include loss of excess ligand in half-met excess N_3^- (Fig. 3) and changes in the half-met–acetate and half-met–SCN^- (Fig. 4) EPR signals to ones similar to the half-met–N_3^- signal. Although the detailed structural implications of these chemical and spectral changes must await further spectral characterization of the pure half-met excess and nonexcess N_3^- forms, two preliminary comments can be made on the basis of our earlier optical and EPR studies:

(*i*) The ability to bind a second ligand in half-met excess N_3^- has been shown (13) to relate to disruption of the endogenous bridging ligand (RO^-) from the Cu(II). The fact that the affinity of the half-met site for this second ligand is greatly reduced in the deoxy quaternary structure indicates that RO^- becomes more sterically competitive at the Cu(II) in the tensed structure.

(*ii*) The half-met–N_3^- EPR signal has been shown (13) to relate to significant delocalization of the extra electron between the two coppers through the bridging azide. The change of this EPR signal upon deoxygenation then indicates that a geometric structural change has occurred at the Cu(II) that allows better overlap of the tetragonal plane with this bridging ligand.

The effective structure of the oxy site shown at the bottom of Fig. 1 is reasonably well defined on the basis of our chemical, spectral, and theoretical studies (11, 12) of the series of derivatives shown in this figure, as well as resonance Raman studies, which indicated (19) the peroxide oxidation state of the bound dioxygen, and extended x-ray absorption fine structure (EXAFS) analysis, which gave a Cu–Cu distance of 3.67 Å (20) or 3.55 Å (21). Cu(I) has a tendency toward lower coordination numbers, softer ligands, and a geometry based on ligand–ligand replusion (rather than unpaired *d* electron effects) relative to Cu(II). One might expect the deoxy site to reflect these tendencies. In addition, the protein must certainly play a role in forming the site, which could result in change in Cu–Cu distance as well as regulation of the endogenous ligand. Earlier speculation (12, 22) has emphasized the potential role of Cu–Cu distance in changing oxygen affinity. Our SP studies presented here demonstrate an important role for the endogenous bridging ligand (RO^-) and have indicated significant geometric changes on the copper ion. Because the d^{10} configuration of the deoxy site is not easily accessible to spectroscopic study, only limited information on this site presently exists. Fourier-transform infrared studies of CO have demonstrated that this ligand binds to only one Cu(I) (23). This could relate to the steric role of the endogenous RO^- ligand at the deoxy site. Further, the two extended x-ray absorption fine structure studies do indicate that the number of ligands per copper goes down upon deoxygenation, but presently disagree on the Cu(I)–Cu(I) distance [3.4 Å (20) vs. >4 Å (24)]. Clearly, further detailed spectral studies of both the half-met and deoxy sites and models are required to define the importance of Cu–Cu distance and the specific role of the endogenous bridge and ligand geometric constraints in regulating the affinity of this site for dioxygen.

D. E. Wilcox, C. D. LuBien, and M. E. Winkler are acknowledged for useful discussions. We are grateful to the National Institute of Arthritis, Diabetes, and Digestive and Kidney Diseases of the U.S. Public Health Service (AM 31450).

1. Lamy, J. & Lamy, J., eds. (1981) *Invertebrate Oxygen-Binding Proteins* (Dekker, New York).
2. Van Holde, K. E. & Van Bruggen, E. F. J. (1971) in *Subunits in Biological Systems*, eds. Timasheff, S. N. & Fasman, G. D. (Dekker, New York), Vol. 5, pp. 1–53.
3. Van Holde, K. E. & Miller, K. (1974) *Biochemistry* **13**, 1668–1674.
4. Brouwer, M., Bonaventura, C. & Bonaventura, J. (1978) *Biochemistry* **13**, 1668–1674.
5. Perutz, M. F. (1970) *Nature (London)* **228**, 726–739.
6. Perutz, M. F. (1979) *Annu. Rev. Biochem.* **48**, 327–386.
7. Collman, J. P. & Suslick, K. S. (1978) *Pure Appl. Chem.* **50**, 951–961.
8. Ogawa, S. & Shulman, R. G. (1971) *Biochem. Biophys. Res. Commun.* **42**, 9–15.
9. Asakura, T. & Droff, H. R. (1971) *Biochem. Biophys. Res. Commun.* **44**, 1199–1204.
10. Perutz, M. F., Sanders, J. K., Chenery, D. H., Noble, R. W., Pennelly, R. R., Fung, L. W. M., Ho, C., Giannini, I., Pörschke, D. & Winkler, H. (1978) *Biochemistry* **17**, 3640–3652.
11. Eickman, N. C., Himmelwright, R. S. & Solomon, E. I. (1979) *Proc. Natl. Acad. Sci. USA* **76**, 2094–2098.
12. Solomon, E. I. (1981) in *Copper Proteins*, ed. Spiro, T. G. (Wiley-Interscience, New York), Vol. 3, pp. 41–108.
13. Himmelwright, R. S., Eickman, N. C. & Solomon, E. I. (1979) *J. Am. Chem. Soc.* **101**, 1576–1586.
14. Bijlholt, M. M. C., Van Bruggen, E. F. J. & Bonaventura, J. (1979) *Eur. J. Biochem.* **95**, 339–405.
15. Himmelwright, R. S., Eickman, N. C., LuBien, C. D. & Solomon, E. I. (1980) *J. Am. Chem. Soc.* **102**, 5378–5388.
16. Witters, R. & Lontie, R. (1975) *FEBS Lett.* **60**, 400–403.
17. Himmelwright, R. S., Eickman, N. C. & Solomon, E. I. (1979) *Biochem. Biophys. Res. Commun.* **86**, 628–634.
18. Mangum, C. P. & Lykkeboe, G. (1979) *J. Exp. Zool.* **207**, 417–430.
19. Freedman, T. B., Loehr, T. S. & Loehr, T. M. (1976) *J. Am. Chem. Soc.* **98**, 2809–2814.
20. Brown, J. M., Powers, L., Kincaid, B., Larrabee, J. A. & Spiro, T. G. (1980) *J. Am. Chem. Soc.* **102**, 4210–4216.
21. Co, M. S., Hodgson, K. O., Eccles, T. K. & Lontie, R. (1981) *J. Am. Chem. Soc.* **103**, 984–986.
22. Bonaventura, C., Bonaventura, J. & Brouwer, M. (1981) in *Invertebrate Oxygen-Binding Proteins*, eds. Lamy, J. & Lamy, J. (Dekker, New York), pp. 677–691.
23. Van Der Deen, H. & Hoving, H. (1979) *Biophys. Chem.* **9**, 169–179.
24. Co, M. S. & Hodgson, K. O. (1981) *J. Am. Chem. Soc.* **103**, 3200–3201.